

# Gamma absorbed radiation dose in Marrah mountain series, western Sudan

Saadeldien Abdalhamid<sup>1</sup> · Isam Salih<sup>2,3</sup>  · Hajo Idriss<sup>2,4</sup>

Received: 18 June 2016 / Accepted: 4 October 2017 / Published online: 12 October 2017  
© Springer-Verlag GmbH Germany 2017

**Abstract** Measurements of ambient gamma radiation dose and radioactivity of soil and rocks samples have been carried out in 103 sites located in the region of Marrah mountain (western Sudan) using survey meters and gamma spectrometry techniques, respectively. The ambient dose varied from 0.05 to 0.25  $\mu\text{Sv/h}$  with mean value of  $0.18 \pm 0.05$  (SD)  $\mu\text{Sv/h}$ . At high altitudes ( $> 1500$  m), relatively high values were observed ( $0.18\text{--}0.22$   $\mu\text{Sv/h}$ ). The levels of  $^{238}\text{U}$ ,  $^{232}\text{Th}$  and  $^{40}\text{K}$  in soil–rocks were in the ranges 12–80, 12–66 and 120–937 Bq/kg with mean  $\pm$  SD of ( $41 \pm 6.9$ ), ( $24 \pm 12$ ) and ( $540 \pm 99$ ) Bq/kg, respectively, equivalent to total gamma absorbed dose of 23–142 ( $66 \pm 20$ ) nGy/h. The ambient dose data were presented in cartography format, and correlation to geological maps was attempted. Surface map of the absorbed dose created using geostatistical kriging tools showed the spatial distribution of dose. Analyses showed that trends of high values were located in and around areas characterized by local flow and basaltic flow lithology, while the low values were observed at locations of basement rocks (granitic) in general. That was attributed to the differences in environmental conditions in various altitude and weathering processes. The

highest readings (0.25  $\mu\text{Sv/h}$  and 142 nGy/h) were found in Deriba Complex Pumice air-fall deposits (younger explosive phase). Health risk was assessed by calculating annual effective dose for the inhabitants resulted in values range between 0.14 and 1.4 mSv/y (mean  $\pm$  SD of  $0.40 \pm 0.12$  mSv/y). The observed values of dose rates are comparable with some countries but higher than the worldwide average for outdoor annual affective dose of 0.07 mSv/y.

**Keywords** Ambient dose · Gamma absorbed dose · Natural radioactivity · Marrah mountain

## Introduction

Assessment of natural radioactivity in populated area surrounded by mountains is of great importance. Environmental radioactivity monitoring leads to evaluating levels and estimating radiation exposure for the inhabitants. It is also useful to gather long-term information on the levels, spatial distributions and trends. Uranium and thorium are useful in nuclear industry if exploration of them intended. However, their presents at high levels may have impact on human health due to internal and/or external exposures. Therefore, there are so many studies conducted at many places worldwide (example of that, the work done by: Paschoa and Godoy 2002; Sartandel et al. 2009; Al-Sulaiti et al. 2012; Saïdou et al. 2011; Popov 2012; Bezuidenhout 2013; Keith et al. 2015 and Idriss et al. 2016). Radioactivity measurements to produce baseline data such as maps and spread sheets are useful for a country in scientific manners. Natural radioactivity in the environment arises mainly from uranium and thorium series in addition to radioactive potassium ( $^{238}\text{U}$ ,  $^{232}\text{Th}$  and  $^{40}\text{K}$ ). These

✉ Isam Salih  
isamsalih@gmail.com

<sup>1</sup> Atomic Energy Council, Sudan Academy of Science, Khartoum, Sudan

<sup>2</sup> Radiation Safety Institute, Sudan Atomic Energy Commission, P.O. Box 3001, Khartoum, Sudan

<sup>3</sup> Present Address: Physics Department, Taibah University, AlMadinah Almunawwarah, Saudi Arabia

<sup>4</sup> Committee on Radiation and Environmental Pollution Protection, Al Imam Mohammad Ibn Saud Islamic University, Riyadh, Saudi Arabia

nuclides pose risks from external exposure due to their gamma-ray emissions, and it can reach very high levels, especially if processed for some industry, e.g., producing fertilizers from phosphate rocks or mining (Makweba and Holm 1993; Sam and Holm 1995; do Rio et al. 2002), which may lead to high exposures to man. Some high-background radiation areas were identified around the world, and many of these high areas located at high altitudes (Mehdi 2013; Aliyu and Ramli 2015; Pooya et al. 2015; Sahoo et al. 2015). That motivated us to continue our radioactivity monitoring program and focus on high places such as Marrah mountain series that is located in Darfur region, western Sudan. Up to our knowledge, this is the first study of its kind intended to assess radioactivity profile in that region. The geology of the area is mostly characterized by various volcanic rocks (called Deriba Complex). The total area of Marrah mountain is about 75,000 km<sup>2</sup> and reaches a height up to 3 km where high rainfall and water springs originate. The area is populated by approximately 1.5 million of inhabitants (majority are farmers and herdsmen) spend most of their time outdoors. Therefore, this study was carried out to characterize and evaluate the levels of natural radioactivity, assess external and effective dose to inhabitants due to gamma radiation in Marrah mountain and to construct map of ambient dose as baseline data for the country.

## Materials and methods

Figure 1 shows the study area in the map of Sudan where the location of 103 sites recorded using a portable global positioning system (GPS). The area is located between (12.00°N–14.21°N) and (22.25°E–25.27°E) with altitudes ranging from 644 to 1999 m above sea level. Geological map of the area is shown in Fig. 2 (extracted from Geological Interpretation Map of Sudan 1:100 000), where main geological classes are identified. Ambient dose measurements were taken using two gamma survey meters Identifinder<sup>TM</sup> and RADOS. The Identifinder instrument functions were based on combined NaI detector (energy range 15 keV–3.0 MeV) and GM detector (energy range 60 keV–1.6 MeV). Beside its function of identifying nuclides, it gives measurements of dose rates (with total dose rate ranging from 0.01 μSv/h to 1 Sv/h). RADOS measures dose rates based on ionization chamber detector (ranging from 0.01 μSv/h to 100 mSv/h). The activity measurements of soil and rocks were taken using standard gamma spectrometry (located at Radiation Safety Institute of Sudan Atomic Energy Commission) where <sup>238</sup>U, <sup>232</sup>Th and <sup>40</sup>K nuclides are evaluated. From location, rock

samples were taken and soil samples were collected using a 10-cm-diameter auger, designed to sample up to 20 cm depth of soil. Two or three soil samples (wherever possible) were collected from each location, put into the plastic bags to ensure that cross-contamination does not occur, sealed, labeled and secured. The samples identification, location, date and time have been recorded on a logbook. Samples were then crumpled into homogeneous small pieces, sieved (through 2 mm sieve), placed in 500-ml Marinelli beakers and stored 3–4 weeks prior to measurement by gamma spectrometry. The specific activities were evaluated with gamma-ray spectrometry by the *p* type high-purity germanium (HPGe) using Gamma 2000 software and 3" × 3" sodium iodide (NaI) scintillation detector systems. Gamma spectrometry system employed for measurements in the present study was composed of 3" × 3" NaI(Tl) detector with built-in preamplifier, amplifier and MCA plugged to a computer through USB connection. The spectra are collected and analyzed using "Win TMCA32 target" GmbH software. The HPGe detector, with a relative efficiency of 20% (FWHM of 1.8 keV at 1773 keV), was calibrated using standard from Amersham<sup>TM</sup> and validated with the IAEA certified Reference Materials RGU-1 and RGTh-1. The activities of <sup>226</sup>Ra, <sup>232</sup>Th and <sup>40</sup>K were computed from the <sup>214</sup>Pb 609 keV, <sup>228</sup>Ac 911 keV and 1460 keV gamma lines, respectively. The activity of <sup>238</sup>U in each sample was estimated based on secular equilibrium assumption. The minimum detectable activity, for a 1000-min counting time, ranged between 0.5 and 10 Bq kg<sup>-1</sup>, for the radionuclides <sup>214</sup>Pb, <sup>228</sup>Ac and <sup>40</sup>K.

Gamma absorbed dose rates in air (at 1 m height from the surface), giving in nGy/h are calculated from the concentration of the three nuclides using the following equation (UNSCEAR 2000):

$$D \text{ (nGy/h)} = 0.461A_U + 0.623A_{Th} + 0.0414A_K \quad (1)$$

where  $A_U$ ,  $A_{Th}$  and  $A_K$  are activity concentrations (given in Bq/Kg) of <sup>238</sup>U, <sup>232</sup>Th and <sup>40</sup>K, respectively.

External hazard index,  $H_{ex}$ , from nuclide concentrations calculated using the formula is given in Eq. 2 as the hazard of the natural gamma radiation (Beretka and Mathew 1985):

$$H_{ex} = \frac{A_U}{370} + \frac{A_{Th}}{259} + \frac{A_K}{4810} \quad (2)$$

Based on the dose values obtained and locations of each sample, surface map of dose rates were created using geostatistical predicting tools in a geographic information system (GIS) software.

**Fig. 1** Map of Sudan showing the locations of the samples of the present study



**Results and discussion**

The goals of the present work were to perform a first-time survey of natural radioactivity measurements of Marrah mountain series, which is located in Darfur region (western Sudan), relate radioactivity to geology and evaluate radiation dose received by inhabitants of the region due to presents of natural radionuclides. Geology of the area is mainly characterized by Deriba Complex—volcanic rocks. Deriba Caldera was formed by explosive eruption of the Marrah mountain volcano about 3500 years ago. The geological formations gave us the motivation to carry out this study where we expect to find spots of high background radiation. The results of 103 measurements taken by portable gamma survey meters and laboratory measurements for collected soil and rock samples (measured using gamma spectrometric techniques) of <sup>238</sup>U, <sup>232</sup>Th and <sup>40</sup>K are presented in tables and figures. Table 1 shows the results of ambient dose measurements categorized according to seven identified geological classes. The highest value (0.25 μSv/h) was observed in Saur-Dalda-Fada complex, while the lowest value was in Alkaline Sand (0.05 μSv/h). Among the geological classes, Deriba complex showed the maximum average value of 0.20 ± 0.02 μSv/h, and sedimentary rocks showed the average value of 0.13 ± 0.02 μSv/h as the minimum average. Ambient dose rates data showed non-normal distribution when tested for normality as shown in the

frequency distribution diagram (Fig. 3). Figure 4 shows the ambient dose results in relation to the geological classes given in Table 1. The absorbed dose rate in air values was in the range from 0.05 to 0.25 μSv/h with mean value of 0.18 ± 0.05 μSv/h. At altitudes greater than 1500 m, relatively high values were observed (0.18–0.22 μSv/h), while at low altitudes, the dose varies between 0.05 and 0.21 μSv/h as presented in Fig. 5. Relatively high values were observed in and around areas characterized by local flow and basaltic flow lithology. The low dose values, however, were observed at basement rocks (granitic) in general. The highest reading (0.25 μSv/h) was in Deriba Complex Pumice air-fall deposits (younger explosive phase).

Analyses of soil and rock samples showed the concentration of <sup>238</sup>U, <sup>232</sup>Th and <sup>40</sup>K, ranging 12–80, 12–66 and 120–937 Bq/kg, and mean values, together with their respective standard deviation (SD), of 41 ± 6.9, 24 ± 12 and 540 ± 99 Bq/kg, respectively. These results are sorted and presented in Table 2 in association with geology where seven geological classes have been identified. The maximum values of uranium (80 Bq/kg) and thorium (66 Bq/kg) are comparable to maximum reported values from other regions (examples of that are reported by Selvasekarapandian et al. 2000; Jeevarenuka et al. 2014; Malczewski et al. 2004; El-Arabi et al. 2006; Abd Elmageed et al. 2011; Alnour et al. 2012; Beamish 2014 and Yildiz et al. 2014). In order to evaluate exposure, the

**Fig. 2** Geological map of the surveyed area

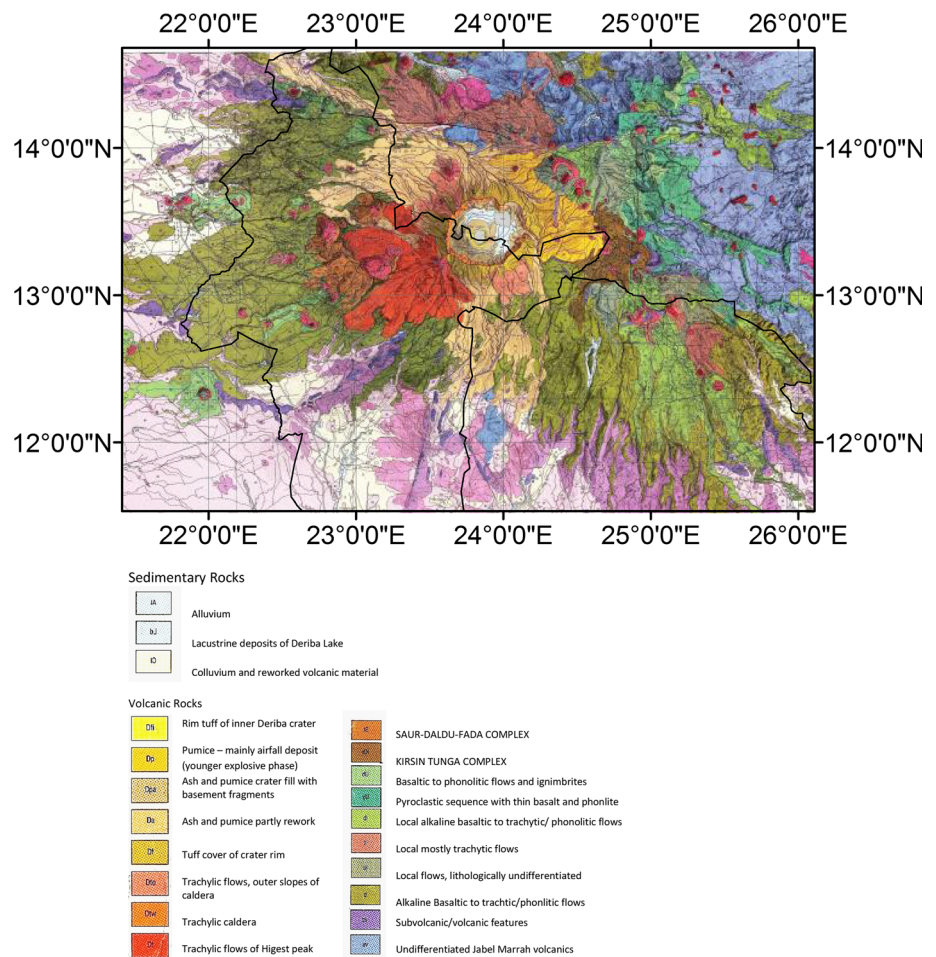


**Table 1** Ambient dose and calculated annual effective dose from different geological backgrounds

Geological group	Number of sites	Ambient gamma dose ( $\mu\text{Sv/h}$ )				Effective dose ( $\text{mSv/y}$ )
		Average	Max	Min	SD	
Sedimentary rocks	6	0.13	0.15	0.11	0.02	$1.1 \pm 0.2$
Deriba complex	27	0.20	0.23	0.15	0.02	$1.8 \pm 0.2$
Saur-Dalda-Fada complex	8	0.19	0.25	0.11	0.05	$1.7 \pm 0.4$
Kirsn Tunga complex	13	0.14	0.22	0.05	0.07	$1.2 \pm 0.6$
Uwa Corogntong complex	8	0.20	0.22	0.12	0.03	$1.8 \pm 0.3$
Subsidiary cones	10	0.14	0.21	0.09	0.04	$1.2 \pm 0.4$
Alkaline sand	31	0.14	0.21	0.05	0.06	$1.2 \pm 0.5$
All groups	103	0.18	0.25	0.05	0.04	$1.4 \pm 0.4$

activity concentration of these nuclides was then converted into absorbed dose rates using Eq. 1. Table 3 shows the average absorbed dose rates ranging from 23 to 142 nGy/h of  $66 \pm 20$  nGy/h. The reported mean dose rates from the above-mentioned regions are also comparable to mean value found in this study. However, the maximum value of this study is higher than reported values from those regions [98 nGy/h in northern Tanzania (Banzi et al. 2002), 55 nGy/h in Egypt (El-Arabi et al. 2006), 112 nGy/h in

Malesia (Alnour et al. 2012), 74 nGy/h in India (Jeevarenuka et al. 2014) and 135 nGy/h in Kashmir (Rafique et al. 2014)]. The maximum value of absorbed dose rate found in this study (142 nGy/h) is lower than the maximum reported value (300 nGy/h) for granitic terrain areas in UK (Beamish 2014). The mean and maximum values of the dose rates were higher when compared to the world average (59 nG/h) and maximum (93 nGy/h) given in the

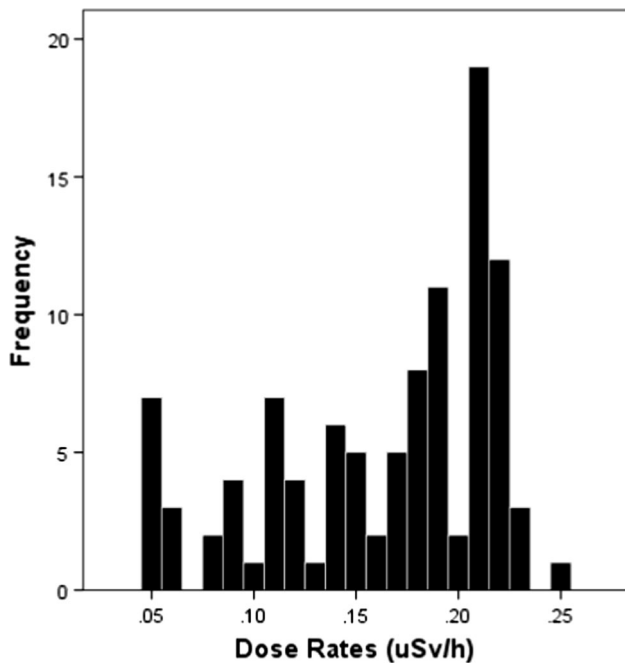


Fig. 3 Histogram of ambient dose rates

United Nations Scientific Committee on the Effect of Atomic Radiation report (UNSCEAR 2000).

The wide range of absorbed dose was found in this study to express the complexity of the radioactivity distribution in the area. In order to see trends, an attempt was made to construct a surface map of gamma radiation dose by creating surface where estimation of unmeasured places was

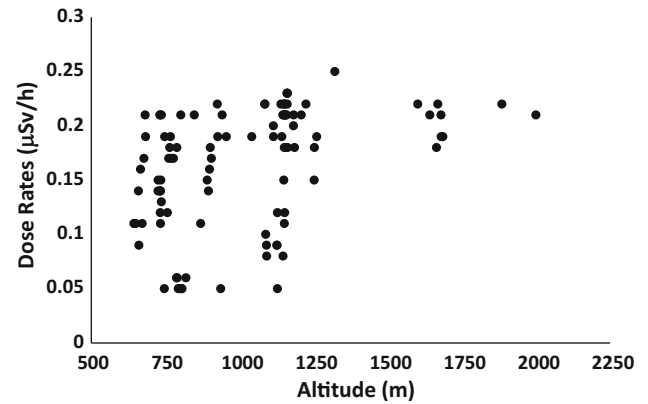


Fig. 5 Dose rates at different altitudes

predicted using a built-in geostatistical tool of kriging in GIS software. Cross-validation performed for this estimation exhibited a root-mean-square error of 23 nGy/h and average standard error of 24.5 nGy/h. Salih et al. 2002 reported the details of the prediction methods (kriging, inverse distance weight, etc.) needed to create a continuous surface from scattered data points. Figure 6 shows the results of the prediction where high levels were observed in areas characterized by basaltic lithology (as compared with Fig. 2).

To limit the external  $\gamma$ -radiation dose and assess hazard risk, the model proposed by Beretka and Mathew (1985), as given in Eq. 2, was used in this study. Table 2 shows the values range between 0.1 and 0.67 with a mean value of  $0.32 \pm 0.09$ , which is less than unity indicating low risks

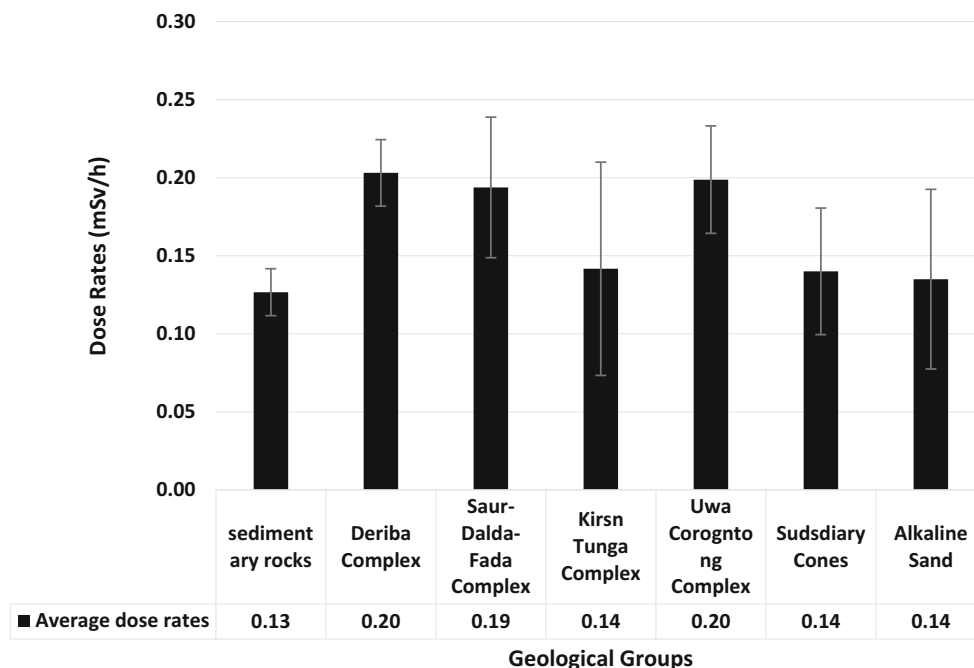


Fig. 4 Results of field measurement of ambient dose ( $\mu$ Sv/h) versus main geological classes



**Table 2** Descriptive statistics of the concentration of  $^{238}\text{U}$ ,  $^{232}\text{Th}$  and  $^{40}\text{K}$  (Bq/kg) in rock and soil samples, calculated absorbed dose rate,  $D$  (nGy/h) and external hazard risk,  $H_{\text{ex}}$ , for all geological classes (summary)

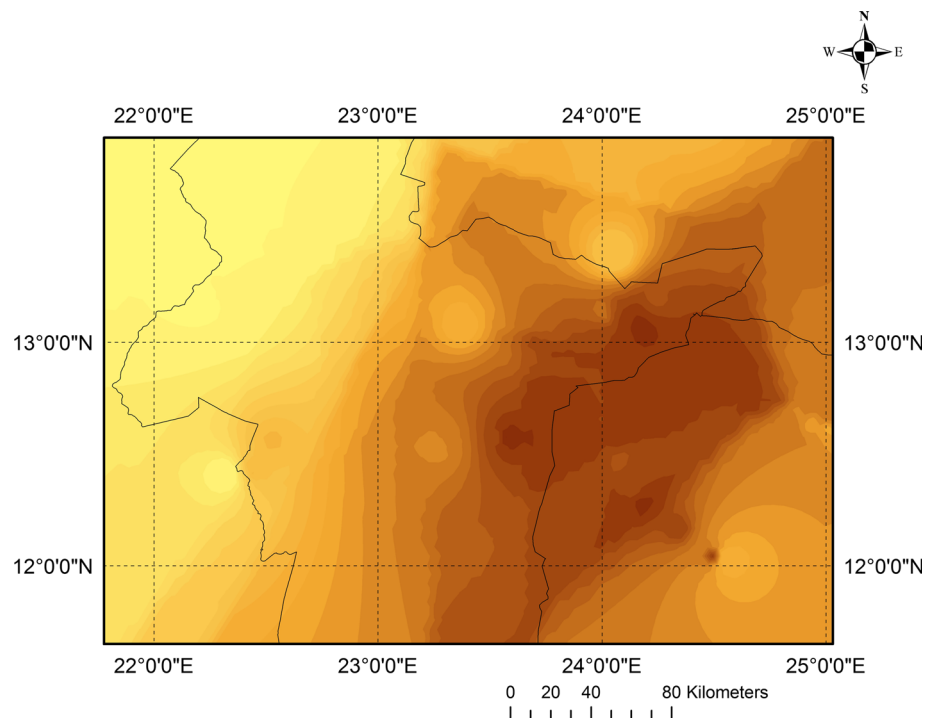
	$^{238}\text{U}$	$^{232}\text{Th}$	$^{40}\text{K}$	$D$ (nGy/h)	$H_{\text{ex}}$
Mean	41	24	540	65.9	0.32
SD	6.9	12	99	19.9	0.09
Min	12	12	120	23.1	0.10
Max	80	66	937	142.3	0.67

**Table 3** Average absorbed dose rate,  $D$  (nGy/h), calculated from radionuclide concentrations and average external hazard risk,  $H_{\text{ex}}$ , for each geological class

Geological group	Average	Dose rate (nGy/h)		$H_{\text{ex}}$
		SD (%)	Range	
Sedimentary rocks	47	24	23–78	0.2
Deriba complex	74	31	55–121	0.4
Saur-Dalda-Fada complex	76	38	65–142	0.4
Kirsn Tunga complex	52	50	37–133	0.3
Uwa Corogntong complex	74	15	47–87	0.4
Subsidiary cones	70	25	32–88	0.4
Alkaline sand	68	15	42–82	0.3

The standard deviation for both quantities (given as percent) ranged between 15 and 50%

**Fig. 6** Surface map showing the spatial distribution of ambient dose predicted from the measurements giving values range from 0.05  $\mu\text{Sv/h}$  (light color) to 0.25  $\mu\text{Sv/h}$  (dark color)



of exposure due to the presence of studied radionuclides at these levels. Table 3 shows average external hazard risk ( $H_{\text{ex}}$ ) categorized according to the geological classes.

The inhabitants of this region spend most of their time outdoors; therefore, the dose calculated here presents actual exposures. (Indoor do not possess additional exposure because most of the houses are built of local forests materials.) Annual effective dose rate in air is estimated using the conversion coefficient of 0.7 Sv/Gy (UNSCEAR 2000), and the effective dose equivalent ( $D_E$ ) is then given by Eq. (3):

$$D_E (\mu\text{Sv/y}) = D (\text{nGy/h}) \times 8766 \times 0.7 \times 10^{-3} \quad (3)$$

The calculations reveal the values of  $D_E$  ranging from 0.14 to 0.87 ( $0.40 \pm 0.12$ ) mSv/y. However, the average annual effective dose calculated from ambient dose measurements (Table 1) for the population is  $1.4 \pm 0.4$  mSv indicating relatively high values. The average values from the study area are higher than the worldwide average for outdoor annual affective dose, 0.07 mSv per year, as reported by UNSCEAR (2000).

The overall results suggest that radiation levels in the area are slightly high and that the created map will help to identify areas of high levels in any future studies.

## Conclusion

Ambient dose (dose rates at 1-m above the ground) and natural radioactivity of soil–rocks were investigated in Marrah mountain, western Sudan. The results obtained indicated that the levels of  $^{238}\text{U}$ ,  $^{232}\text{Th}$  and  $^{40}\text{K}$  ranges (mean  $\pm$  SD) were 12–80 ( $41 \pm 6.9$ ), 12–66 ( $24 \pm 12$ ) and 120–937 ( $540 \pm 99$ ) Bq/kg, respectively, resulting in equivalent total gamma absorbed dose rate of 23–142 ( $66 \pm 20$ ) nGy/h. The ambient dose ranged from 0.05 to 0.25  $\mu\text{Sv/h}$  with a mean value of  $0.18 \pm 0.05 \mu\text{Sv/h}$ . The average annual effective dose for the inhabitants was calculated to be  $1.4 \pm 0.4 \text{ mSv}$ . The data presented in this survey give a first preliminary result obtained from Darfur region, which is useful as a guide for further studies. Geographic information system (GIS) to create surfaces is found useful to identify trends.

## References

- Abd El-mageed AI, El-Kamel AH, Abbady A, Harb S, Youssef AMM, Saleh II (2011) Assessment of natural and anthropogenic radioactivity levels in rocks and soils in the environments of Juban town in Yemen. *Radiat Phys Chem* 80(6):710–715
- Aliyu AS, Ramli TA (2015) The world's high background natural radiation areas (HBNRAs) revisited: a broad overview of the dosimetric, epidemiological and radiobiological issues. *Radiat Meas* 73(2015):51–59
- Almour IA, Wagiran H, Ibrahim N, Laili Z, Omar M, Hamzah S, Idi Bello Y (2012) Natural radioactivity measurements in the granite rock of quarry sites, Johor Malaysia. *Radiat Phys Chem* 81(12):1842–1847
- Al-Sulaiti H, Nasir T, AlMugren KS, Alkhomashi N, Al-Dahan N, Al-Dosari M, Bradley DA, Bukhari S, Matthews M, Regan PH, Santawamaitre T, Malain D, Habib A (2012) Determination of the natural radioactivity levels in north west of Dukhan, Qatar using high-resolution gamma-ray spectrometry. *Appl Radiat Isot* 70:1344–1350
- Banzi FP, Msaki P, Makundi IN (2002) A survey of background radiation dose rates and radioactivity in Tanzania. *Health Phys* 82(1):80–86
- Beamish D (2014) Environmental radioactivity in the UK: the airborne geophysical view of dose rate estimates. *J Environ Radioact* 138:249–263
- Beretka J, Mathew PJ (1985) Natural radioactivity of Australian building materials, industrial wastes and by-products. *Health Phys* 48:87–95
- Bezuidenhout J (2013) Measuring naturally occurring uranium in soil and minerals by analysing the 352 keV gamma-ray peak of  $^{214}\text{Pb}$  using a NaI(Tl)-detector. *Appl Radiat Isot* 80:1–6
- do Rio MAP, Amaral ECS, Fernandes HM, Rochedo EPR (2002) Environmental radiological impact associated with non-uranium mining industries: a proposal for screening criteria. *J Environ Radioact* 59(1):1–17
- El-Arabi AM, Abbady Adel GE, Hussein AS (2006) Gamma-ray measurements of natural radioactivity in sedimentary rocks from Egypt. *Nucl Sci Tech* 17(2):123–128
- Idriss H, Salih I, Alaamer AS, Saleh A, Abdelgali MY (2016) Environmental-impact assessment of natural radioactivity around a traditional mining area in Al-Ibedia, Sudan. *Archives Environ Contam Toxicol* 70(4):783–792
- Jeevarenuka K, Sankaran PG, Hameed PS, Mathiyarasu R (2014) Evaluation of natural gamma radiation and absorbed gamma dose in soil and rocks of Perambalur district (Tamil Nadu, India). *J Radioanal Nucl Chem* 302:245–252
- Keith LS, Faroon OM, Fowler BA (2015) Handbook on the toxicology of metals, 4th edn. Elsevier, pp. 1307–1345
- Makweba M, Holm E (1993) The natural radioactivity of rock phosphates, phosphatic products and their environmental implications. *Sci Total Environ* 133(1–2):99–110
- Malczewski D, Teper L, Dorda J (2004) Assessment of natural and anthropogenic radioactivity levels in rocks and soils in the environs of Swieradow Zdrojin Sudetes, Poland, by in situ gamma-ray spectrometry. *J Environ Radioact* 73:233–245
- Sohrabi M (2013) World high background natural radiation areas: need to protect public from radiation exposure. *Radiat Meas* 50:166–171
- Paschoa AS, Godoy JM (2002) The areas of high natural radioactivity and TENORM wastes. *Int Congr Ser* 1225:3–8
- Pooya Hosseini SM, Dashtipour MR, Enferadi A, Orouji T (2015) Public exposure due to external gamma background radiation in boundary areas of Iran. *J Environ Radioact* 147:97–99
- Popov L (2012) Method for determination of uranium isotopes in environmental samples by liquid–liquid extraction with tri-n-octylamine/xylene in hydrochloric media and alpha spectrometry. *Appl Radiat Isot* 70(10):2370–2376
- Rafique M, Khan AR, Jabbar A, Rahman SU, Kazmi SJA, Nasir T, Arshed W, Matiullah (2014) Evaluation of radiation dose due to naturally occurring radionuclides in rock samples of different origins collected from Azad Kashmir. *Russ Geol Geophys* 55(9):1103–1112
- Sahoo SK, Žunić ZS, Kritsanuwat R, Zagrodzki P, Bossew P, Veselinovic N, Mishra S, Yonehara H, Tokonami S (2015) Distribution of uranium, thorium and some stable trace and toxic elements in human hair and nails in Niška Banja Town, a high natural background radiation area of Serbia (Balkan region, South–East Europe). *J Environ Radioact* 145:66–77
- Saïdou FO, Baechler SB, Moïse KN, Merlin N, Froidevaux P (2011) Natural radioactivity measurements and dose calculations to the public: case of the uranium-bearing region of Poli in Cameroon. *Radiat Meas* 46:254–260
- Salih I, Pettersson HBL, Lund E, Sivertun Å (2002) Spatial correlation between radon ( $^{222}\text{Rn}$ ) in groundwater and bedrock uranium ( $^{238}\text{U}$ ): GIS and geostatistical analyses. *J Spat Hydrol* 2(2):1–10
- Sam A, Holm E (1995) The natural radioactivity in phosphate deposits from Sudan. *Sci Total Environ* 162(2–3):173–178
- Sartandel SJ, Jha SK, Bara SV, Tripathi RM, Puranik VD (2009) Spatial distribution of uranium and thorium in the surface soil around proposed uranium mining site at Lambapur and its vertical profile in the Nagarjuna Sagar Dam. *J Environ Radioact* 100(10):831–834
- Selvasekarapandian S, Sivakumar R, Manikandan NM, Meenakshisundaram V, Raghunath VM, Gajendran V (2000) Natural radionuclide distribution in soils of Gudalore, India. *Appl Radiat Isot* 52:299–306
- UNSCEAR (2000) Effects of atomic radiation to the general assembly. United Nations scientific committee on the effect of atomic radiation, New York
- Yildiz N, Oto B, Turhan S, Ugur FA, Goren E (2014) Radionuclide determination and radioactivity evaluation of surface soil samples collected along the Erçek Lake basin in eastern Anatolia, Turkey. *J Geochem Explor* 146:34–39